



Magnetic loading of TiO₂/SiO₂/Fe₃O₄ nanoparticles on electrode surface for photoelectrocatalytic degradation of diclofenac

Xinyue Hu, Juan Yang, Jingdong Zhang*

College of Chemistry and Chemical Engineering, Huazhong University of Science and Technology, Luoyu Road 1037, Wuhan 430074, PR China

ARTICLE INFO

Article history:

Received 26 May 2011

Received in revised form 29 August 2011

Accepted 5 September 2011

Available online 10 September 2011

Keywords:

TiO₂/SiO₂/Fe₃O₄

Magnetic loading

Photoelectrocatalysis

Diclofenac

ABSTRACT

A novel magnetic nanomaterials-loaded electrode developed for photoelectrocatalytic (PEC) treatment of pollutants was described. Prior to electrode fabrication, magnetic TiO₂/SiO₂/Fe₃O₄ (TSF) nanoparticles were synthesized and characterized by X-ray diffraction (XRD), transmission electron microscopy (TEM) and FT-IR measurements. The nanoparticles were dispersed in ethanol and then immobilized on a graphite electrode surface with aid of magnet to obtain a TSF-loaded electrode with high photoelectrochemical activity. The performance of the TSF-loaded electrode was tested by comparing the PEC degradation of methylene blue in the presence and absence of magnet. The magnetically attached TSF electrode showed higher PEC degradation efficiency with desirable stability. Such a TSF-loaded electrode was applied to PEC degradation of diclofenac. After 45 min PEC treatment, 95.3% of diclofenac was degraded on the magnetically attached TSF electrode.

© 2011 Elsevier B.V. All rights reserved.

1. Introduction

Over past decades, TiO₂ has been extensively utilized as an efficient photocatalyst for the removal of pollutants from wastewater [1,2]. However, practical applications of slurry photocatalyst to wastewater treatment are usually limited because a costly and difficult post-treatment process is required to separate slurry TiO₂ from treated water. To overcome this problem, magnetically separable composite photocatalysts such as TiO₂/Fe₃O₄ and TiO₂/SiO₂/Fe₃O₄ (TSF) have been prepared and applied to the degradation of pollutants [3–7]. Alternatively, preparation of TiO₂ film by immobilizing photocatalyst onto various solid supports has also been considered as an effective method to overcome the separation problem of slurry TiO₂ [8–13]. Unfortunately, the immobilized TiO₂ film reduces the reaction surface area of catalyst and thus decreasing the degradation efficiency, as compared with the slurry catalyst. To improve the photocatalytic efficiency of TiO₂ film, photoelectrocatalytic (PEC) technique by applying an external bias potential on TiO₂ film-coated electrode has been developed [14].

For PEC electrode, the catalyst must be firmly adhered to the solid support to keep high stability of electrode and allow facile electron transfer between catalyst and electrode. Traditional PEC electrodes prepared from TiO₂ sol-gel are generally treated

with high temperature to reinforce the adherence of catalyst to the electrode surface [15–18]. Recently, magnetic loading has been developed for constructing electrochemical sensors [19,20]. To prepare magnetic electrode, magnetic Fe₃O₄-SiO₂ core-shell bio-nanoparticles have been prepared and immobilized on the electrode surface with the help of magnetic force [21]. A novel electrochemical-sensing platform based on the magnetic loading of CNT/Fe₃O₄ composite on electrodes for the detection of hydrogen peroxide has been demonstrated [22].

As a group of emerging contaminants, pharmaceuticals and personal care products (PPCPs) have received considerable attention in recent years. PPCPs are regarded as potentially hazardous compounds since many of them are ubiquitous, persistent and biologically active compounds with endocrine disruption functions [23]. Diclofenac is a widely used non-steroidal anti-inflammatory drug. It has been one of the most frequently detected PPCPs in water environment at concentrations up to 1.2 µg/L [24]. Advanced oxidation processes such as photocatalysis [24], UV [25], UV/H₂O₂ [26], photo-Fenton [27,28], ozonation [26,29,30], and sonolysis [31,32] have been applied to the removal of diclofenac from polluted water.

In this work we reported a novel magnetic composite nanomaterials-loaded electrode with photoelectrochemical activity, which was fabricated by immobilizing TSF nanoparticles on the electrode surface with aid of magnet. The magnetic force between external magnet and TSF nanoparticles allowed a desirable adherence of catalyst to the electrode. Such a TSF-loaded electrode was successfully applied to the PEC degradation of diclofenac.

* Corresponding author. Tel.: +86 27 87792154; fax: +86 27 87543632.

E-mail address: zhangjd@mail.hust.edu.cn (J. Zhang).

2. Experimental

2.1. Chemicals

$\text{FeCl}_3 \cdot 6\text{H}_2\text{O}$, $\text{FeSO}_4 \cdot 7\text{H}_2\text{O}$, tetraethoxysilane (TEOS), tetrabutyl orthotitanate (TBOT), sodium dodecyl sulfate (SDS), methylene blue (MB) and Na_2SO_4 were obtained from Sinopharm chemical Reagent Co. (Shanghai, China). Diclofenac sodium was obtained from Sigma Chemical Reagent Co., USA. Multi-walled CNTs (diameter 20–30 nm, length 1–10 μm) provided by Nanjing University (Nanjing, China) were pretreated in a mixture of concentrated nitric acid/sulfuric acid (1:3, v/v) with ultrasonication for 8 h, swilled to neutral and then dried at 60 °C. Other chemicals such as HCl, H_2SO_4 , $\text{NH}_3 \cdot \text{H}_2\text{O}$ (25 wt%), NaAc, HAc, Na_2HPO_4 , NaH_2PO_4 , dimethylformamide (DMF), cetyltrimethylammonium bromide (CTAB) and ethanol were of analytical grade. Doubly distilled water was used in all experiments.

2.2. Preparation of Fe_3O_4 , $\text{SiO}_2/\text{Fe}_3\text{O}_4$ and TSF nanoparticles

The magnetite nanoparticles were prepared by the coprecipitation method. Typically, 60 mL mixture of iron salts with a molar ratio ($\text{FeCl}_3 : \text{FeSO}_4$) of 1:2 was prepared in the presence of 0.5% SDS. A concentrated solution of 25 wt% $\text{NH}_3 \cdot \text{H}_2\text{O}$ was added drop-by-drop with stirring until pH 10. The reaction mixture was heated at 40 °C for 30 min, then separated with magnet and swilled to neutral. The obtained Fe_3O_4 particles were washed with ethanol for three times followed by drying at 80 °C under vacuum for 11 h.

$\text{SiO}_2/\text{Fe}_3\text{O}_4$ (SF) was prepared using a modified sol–gel process. In this process, a suspension of the synthesized Fe_3O_4 nanoparticles (0.4 g) was diluted by a mixture of the precursor of TEOS (11 mL) and ethanol (60 mL), followed by the drop-by-drop addition of a mixture of 25 wt% $\text{NH}_3 \cdot \text{H}_2\text{O}$ (8 mL) and ethanol (40 mL) with stirring at room temperature for 6 h. The product was separated with magnet, washed with ethanol and dried at 60 °C for 8 h.

Coating SF with TiO_2 was also carried out using the sol–gel technique. Briefly, the suspension with SF particles (0.5 g), TBOT (5 mL) and ethanol (20 mL) was prepared and ultrasonic for 10 min. Then, a mixture of 1.5 mL H_2O , 0.1 mL hydrochloric acid and 20 mL ethanol was added drop-wise to the SF suspension under vigorous stirring at 40 °C until gel was formed. The product was dried at 80 °C to evaporate ethanol, and then ground into powder and calcined at 450 °C for 1 h.

2.3. Preparation of magnetically attached TSF electrode

Typically 50 mg of TSF was dispersed in 1 mL of ethanol to give a 50 mg/mL suspension with the aid of ultrasonic agitation. Prior to modification, the graphite electrode surface (2 cm \times 4 cm) was polished with emery papers, ultrasonically washed in ethanol and distilled water for several minutes and then dried with nitrogen gas. A Nd–Fe–B magnet (3500 Gauss, 2 cm \times 4 cm \times 0.5 cm, Ying-shen Magnet Co., China) enwrapped with a layer of PVC thin film was glued to the back of the working surface of graphite and then 120 μL of 50 mg/mL TSF suspension was coated on the working surface of electrode and dried in air. The PVC film could avoid the contact of magnet with solution when the magnetically attached TSF electrode was utilized in electrolyte solution.

2.4. Apparatus and procedures

XRD patterns were measured using a diffractometer (X' pert PRO, PANalytical B.V., the Netherlands) with radiation of a Cu target ($K\alpha$, $\lambda = 0.15406 \text{ nm}$). TEM observation was performed on a JEM-100CXII TEM instrument (JOEL Ltd., Japan) operated at a 100 kV

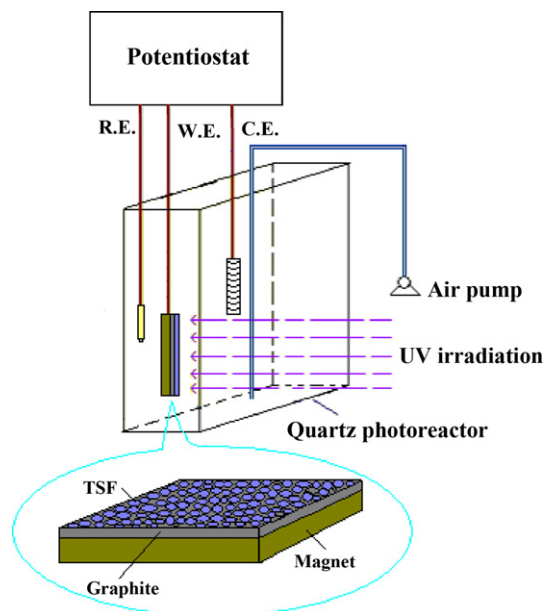


Fig. 1. Diagram of PEC degradation experimental setup using magnetically attached TSF electrode.

accelerating voltage. The FT-IR spectra were measured with an Equinox 55 FTIR spectrophotometer (Bruker Co., Germany). The concentration of MB was measured by monitoring the absorbance at the maximum absorption wavelength at 660 nm with a UV-2000 UV-visible spectrometer (Shanghai Unico Instruments Co., China).

The PEC degradation experiments were performed in a quartz photoreactor containing 100 mL sample solution. The magnetically attached TSF electrode was placed in the photoreactor as the working electrode (W.E.). A platinum wire and a saturated calomel electrode (SCE) were used as the counter electrode (C.E.) and reference electrode (R.E.), respectively. All the potentials were versus SCE. The electrochemical measurements were carried out using a CHI 660A potentiostat (Shanghai Chenhua Instrument Co., China). A 15 W low pressure Hg lamp with a major emission wavelength of 253.7 nm was used for UV irradiation. The experimental setup for PEC degradation of pollutants was illustrated in Fig. 1.

The voltammetric measurements were performed in a 10 mL conventional three-electrode electrolytic cell. A CNT-modified glassy carbon electrode described as our previous report [33], a platinum wire and a SCE served as the working, auxiliary and reference electrodes, respectively. For voltammetric analysis of degraded diclofenac, 1.0 mL sample was taken out of the photoreactor, and diluted with 8.0 mL doubly distilled water and 1.0 mL of 1.0 mol/L H_2SO_4 , and then analyzed in the electrolytic cell using the CNT-modified electrode. The chemical oxygen demand (COD) value was determined using the traditional dichromate method [33].

LC/MS analysis was carried out in a Finnigan LTQ XL linear ion trap mass spectrometer (Thermo Fisher, USA). The degradation product of diclofenac was separated by Ultimate 3000 (Donex, USA) liquid chromatography using an Acclaim 120 C18 column, 250 mm \times 4.6 mm, with 60–80% CH_3CN (0–7 min), 80% CH_3CN (7–25 min) as eluent. The flow rate was 2.5 mL/min. The detection wavelength was set at 365 nm. The mass spectrometer was equipped with an electrospray ionization (ESI) source. The source voltage was set at the 3.5 kV value. The tuning parameters adopted for ESI source were the following: source current 100.00 μA , capillary voltage –35.00 V, capillary temperature 250.00 °C, tube lens offset –200.00 V, sheath gas flow 20.00 L/min, auxiliary gas flow 6.00 L/min.

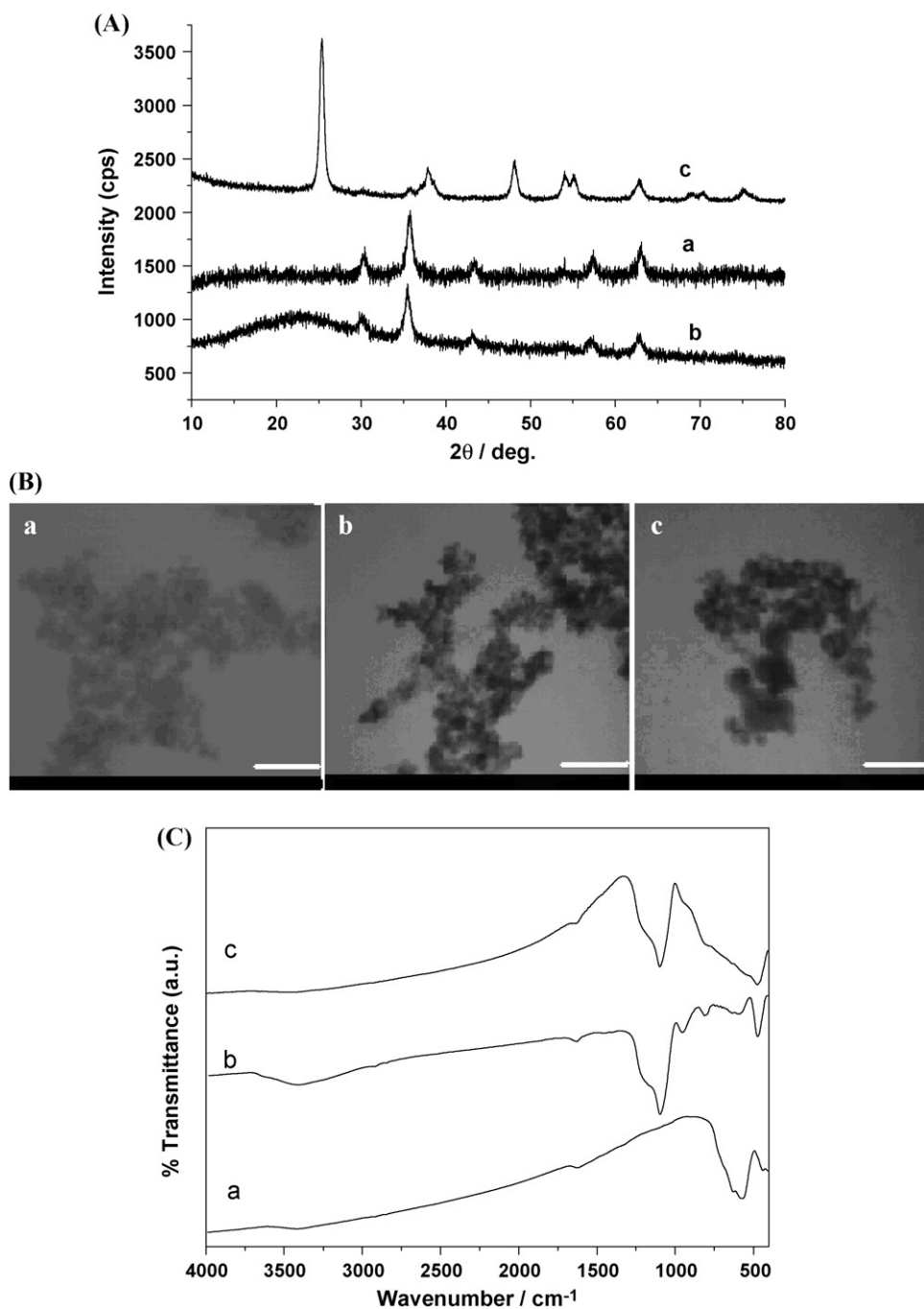


Fig. 2. (A) XRD patterns, (B) TEM images and (C) FT-IR spectra for Fe_3O_4 (a), SF (b) and TSF (c) nanoparticles (bar: 140 nm).

3. Results and discussion

3.1. Surface characterization of TSF nanoparticles

Fig. 2A shows the XRD patterns for pure Fe_3O_4 , SF and TSF nanoparticles. As can be seen, the characteristic peaks at $2\theta = 30.4^\circ$, 35.6° , 43.2° , 53.8° , 57.2° and 62.9° for pure Fe_3O_4 nanoparticles agree well with those XRD patterns of Fe_3O_4 nanoparticles in the literature [34–36], indicating a cubic spinel structure of magnetite. The XRD pattern of SF particles is similar to the pattern of Fe_3O_4 but shows an obvious diffusion peak at $2\theta = 15\text{--}25^\circ$, generally considered as the diffusion peak of amorphous silica. For the sample of TSF particles, several diffraction peaks at 25.4° , 37.8° , 48.1° , 54.1° , 55.2° , 68.8° , 70.3° , 75.2° reveal the formation of anatase TiO_2 . At the

same time, the TEM images of three types of prepared particles are shown in Fig. 2B, which indicate the diameter of Fe_3O_4 nanoparticles are increased after it is coated with SiO_2 layer. While the second layer of TiO_2 is coated on SF, the size of nanoparticles is further enlarged up to 120 nm. Fig. 2C compares the FT-IR spectra of these particles. For Fe_3O_4 , the absorption band at 568 cm^{-1} corresponds to the Fe–O vibration from the magnetite phase [37]. While SiO_2 is coated on Fe_3O_4 , the absorption bands at 1093 , 807 , 466 cm^{-1} are observed due to the stretching and deformation vibrations of Si–O–Si. For TSF, the absorption bands in the range from 500 to 900 cm^{-1} relating to the stretching vibration of Ti–O–Ti bond are clearly observed while the band at 1093 cm^{-1} corresponding to the asymmetric stretching vibration of Si–O–Si disappears due to the coat of TiO_2 in the outlayer.

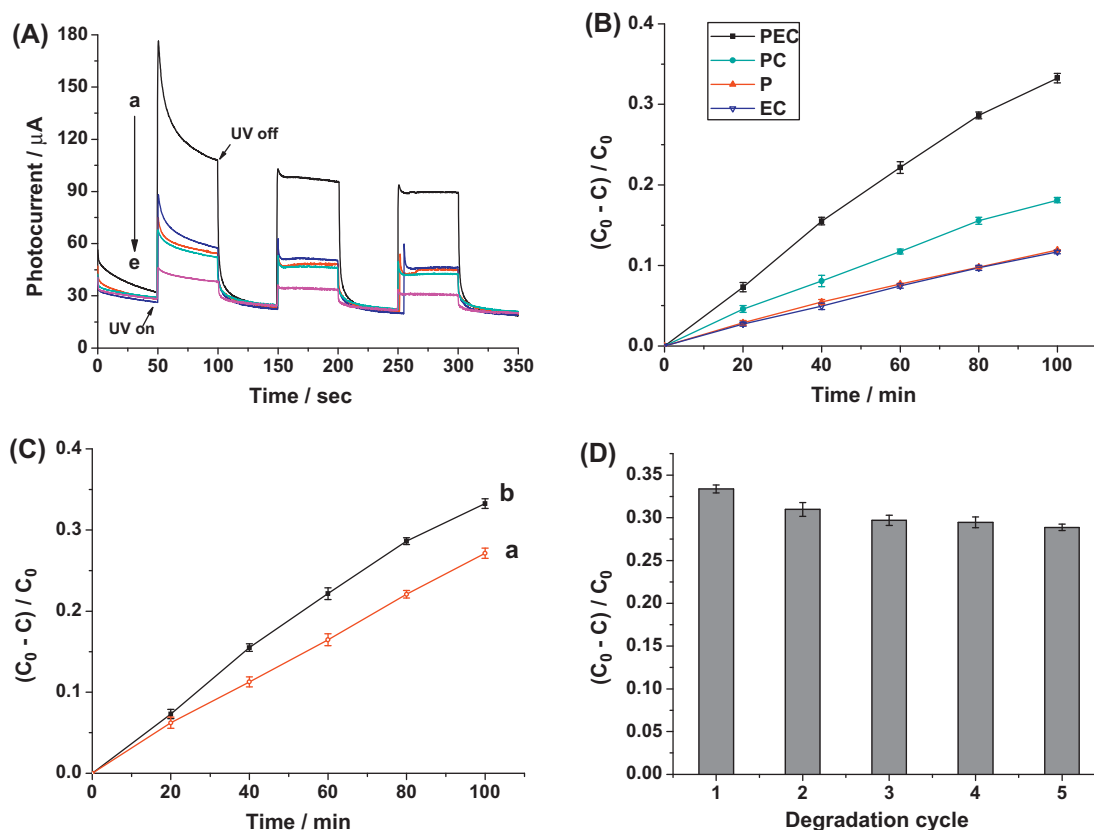


Fig. 3. (A) Effect of different dispersants including (a) ethanol, (b) DMF, (c) 0.5% CTAB, (d) 0.5% SDS and (e) water on the photocurrent response of magnetically attached TSF electrode in 0.1 mol/L Na_2SO_4 at a bias potential of +0.8 V. (B) Comparison of MB degradation efficiency by different processes. PEC: UV + TSF + 0.8 V; PC: UV + TSF; EC: TSF + 0.8 V; P: UV. (C) Degradation curves of magnetically attached TSF electrode without (a) and with (b) magnet. (D) 100 min degradation efficiencies for MB in successive degradation cycles using the magnetically attached TSF electrode. Error bars were derived from three repeated measurements.

3.2. PEC activity of magnetically attached TSF electrode

To obtain a high-performance TSF electrode, the influence of different dispersants such as 0.5% SDS, 0.5% CTAB, DMF, water and ethanol on the photocurrent response of magnetically attached TSF electrodes was measured in an aqueous solution of 0.1 mol/L Na_2SO_4 by applying +0.8 V anodic bias potential. As shown in Fig. 3A, the result clearly indicates that all these magnetically attached TSF electrodes sensitively respond to the UV illumination. However, the response is dispersant-dependent. The photocurrent is only ca. 15 μA on the electrode coated with water-dispersed TSF. While DMF, 0.5% SDS, or 0.5% CTAB was used as dispersant instead of pure water, the photocurrent is improved to ca. 30 μA . The photocurrent response is dramatically improved to ca. 85 μA on the TSF-loaded electrode prepared using ethanol as dispersant. This difference arises from the dispersion of TSF nanoparticles. In aqueous suspension, TSF nanoparticles tend to aggregate due to their high surface energy [38]. The aggregation of TSF nanoparticles reduces the surface area of catalyst to absorb UV illumination, leading to low photocurrent response. When surfactants such as SDS and CTAB are present in suspension, surfactant molecules adsorbed to TSF nanoparticles diminish the aggregation of nanoparticles by modifying their electrostatic, hydrophobic and steric interactions [39]. While TSF is dispersed in DMF, this organic solvent with high dielectric constant forms an electrical double-layer structure on TiO_2 , which decreases the interfacial surface energy and improves the dispersibility of TSF nanoparticles [40]. In comparison, ethanol is the most efficient dispersant for ultrafine TSF nanoparticles due to the formation of a solvent layer on the particle surface which markedly reduces the repulsive potentials between

particles [41,42]. Accordingly, ethanol was selected as the dispersant to prepare TSF electrodes in the following degradation experiments.

MB is an effective organic dye for evaluating the photocatalytic (PC) or PEC activity of semiconductor materials. Thus, the PEC degradation performance of TSF-loaded electrode was investigated using MB as the model pollutant. The degradation experiments were carried out in a solution containing 0.1 mol/L Na_2SO_4 and 5 mg/L MB. Fig. 3B compares the PEC removal of MB on the magnetically attached TSF electrode with other degradation techniques such as photocatalysis (PC), electrochemical oxidation (EC), and direct photolysis (P). The results are described as the variation of the removal efficiency $(C_0 - C) / C_0$ with degradation time t , where C_0 is the initial concentration of MB, and C is the concentration of MB at time t . It is found that the 100 min removal efficiencies for MB by PC, EC and P processes are 18.1%, 11.7% and 11.9%, respectively. In comparison, the PEC process provides the most efficient way to the degradation of MB. By PEC, 33.4% of MB is degraded after 100 min treatment.

The role of magnetic loading was clarified by comparing the degradation efficiencies for MB on TSF electrodes with and without an external magnet (Fig. 3C). It is observed that at the initial degradation time less than 20 min, the difference between two degradation curves is not noticeable. However, with further increasing the degradation time, the magnetically attached TSF electrode shows obviously higher degradation efficiency. For example, the 100 min degradation efficiency of MB on the TSF electrode without magnet is only 27.3%; whereas the efficiency is improved to 33.4% on the magnetically attached TSF electrode. This difference can be attributed to the good adherence of TSF nanoparticles

to the electrode surface by the attraction of magnet. While in the absence of magnet, many TSF particles peel off from the electrode surface during the long-time PEC degradation process, leading to the reduced degradation efficiency. To check the stability of the magnetically attached TSF electrode, several successive PEC degradation experiments were carried out. As can be seen from Fig. 3D, the degradation efficiency only shows a slight decrease in several PEC degradation cycles, demonstrating the desired stability of such a magnetically attached TSF electrode. Moreover, the graphite electrode was also stable and we did not observe dissolution of graphite during the long-time degradation process. Thus, graphite electrode was selected as support for TSF loading.

3.3. Application of magnetically attached TSF electrode to the PEC degradation of diclofenac

The magnetically attached TSF electrode was applied to study the PEC degradation of diclofenac. Considering that diclofenac was an electroactive molecule and CNT-based voltammetry could provide a cheap and useful analytical tool for studying the pollution control [33,43], we developed a voltammetric method using a CNT-modified electrode to monitor the degradation of diclofenac during the PEC treatment. Fig. 4A shows the voltammetric response recorded on the CNT-modified electrode, which

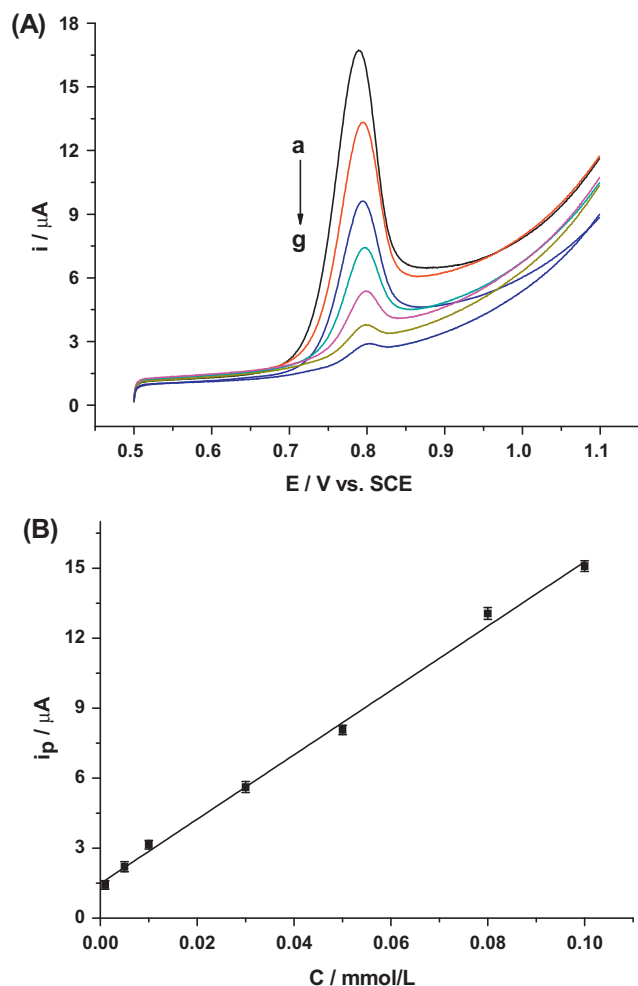


Fig. 4. (A) Linear sweep voltammograms of 0.1 mol/L H_2SO_4 solution containing (a) 1.0×10^{-4} mol/L, (b) 8.0×10^{-5} mol/L, (c) 5.0×10^{-5} mol/L, (d) 3.0×10^{-5} mol/L, (e) 1.0×10^{-5} mol/L, (f) 5.0×10^{-6} mol/L and (g) 1.0×10^{-6} mol/L diclofenac on CNT-modified electrode at 20 mV/s. (B) Linear relationship between the concentration of diclofenac and peak current. Error bars were derived from three repeated measurements.

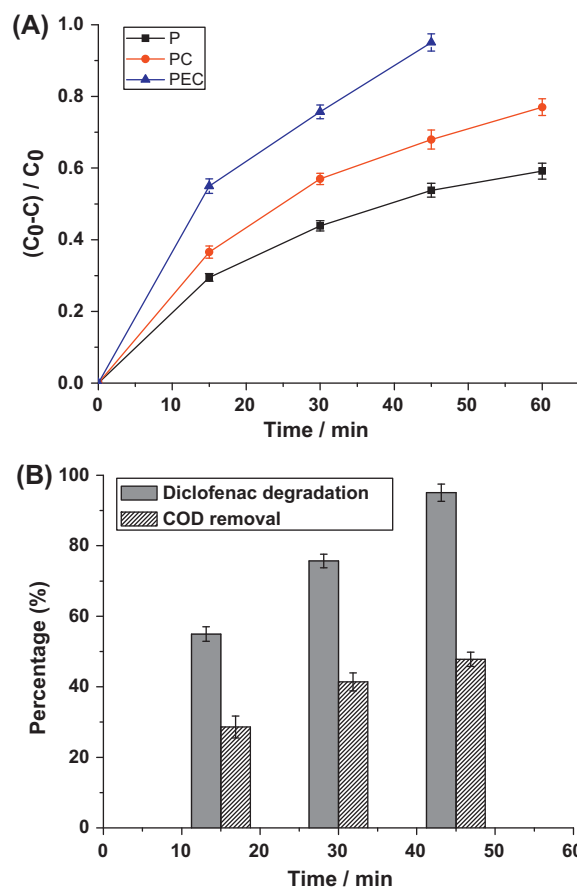


Fig. 5. (A) Degradation efficiency curves for 1.0×10^{-3} mol/L diclofenac in 0.1 mol/L Na_2SO_4 with different techniques. (B) Comparison between COD removal efficiency and diclofenac degradation efficiency treated by PEC technique. Error bars were derived from three repeated measurements.

is linearly increased with the concentration of diclofenac from 1.0×10^{-6} to 1.0×10^{-4} mol/L (Fig. 4B). The linear regression equation is expressed as $i_p(\mu\text{A}) = 1.479 + 138.6c$ (mmol/L) (correlation coefficient $r = 0.9963$). Such a calibration curve was employed to evaluate the degradation efficiency of diclofenac. Typically, diclofenac was degraded on the TSF electrode for appropriate time, and then 1.0 mL of sample was taken out of the reactor and added in electrolytic cell containing suitable supporting electrolyte to analyze the concentration of diclofenac by voltammetric measurement on the CNT-modified electrode. Fig. 5A illustrates the degradation efficiency curves for 1.0×10^{-3} mol/L diclofenac with different techniques. The result indicates that 59.1% of diclofenac is degraded after 60 min UV irradiation. When the magnetically attached TSF electrode is employed to degrade diclofenac, the degradation efficiency reaches 77.3% after 60 min UV irradiation, meaning the photocatalysis of TSF film towards diclofenac. While +0.8V and UV irradiation are simultaneously applied on the magnetically attached TSF electrode, the degradation efficiency of diclofenac is improved to 95.3% after 45 min treatment, indicating the effective PEC degradation of diclofenac on this magnetic electrode. However, the COD removal efficiency is only 47.8% after 45 min PEC treatment (Fig. 5B), almost half of the degradation efficiency. The difference between the degradation efficiency determined by voltammetry and COD analysis indicates that mineralization of diclofenac is slow and many diclofenac molecules are quickly degraded to form intermediates during the PEC process. Thus, prolonging the PEC treatment time is necessary for further oxidation of diclofenac and its degradation intermediates to achieve the complete mineralization.

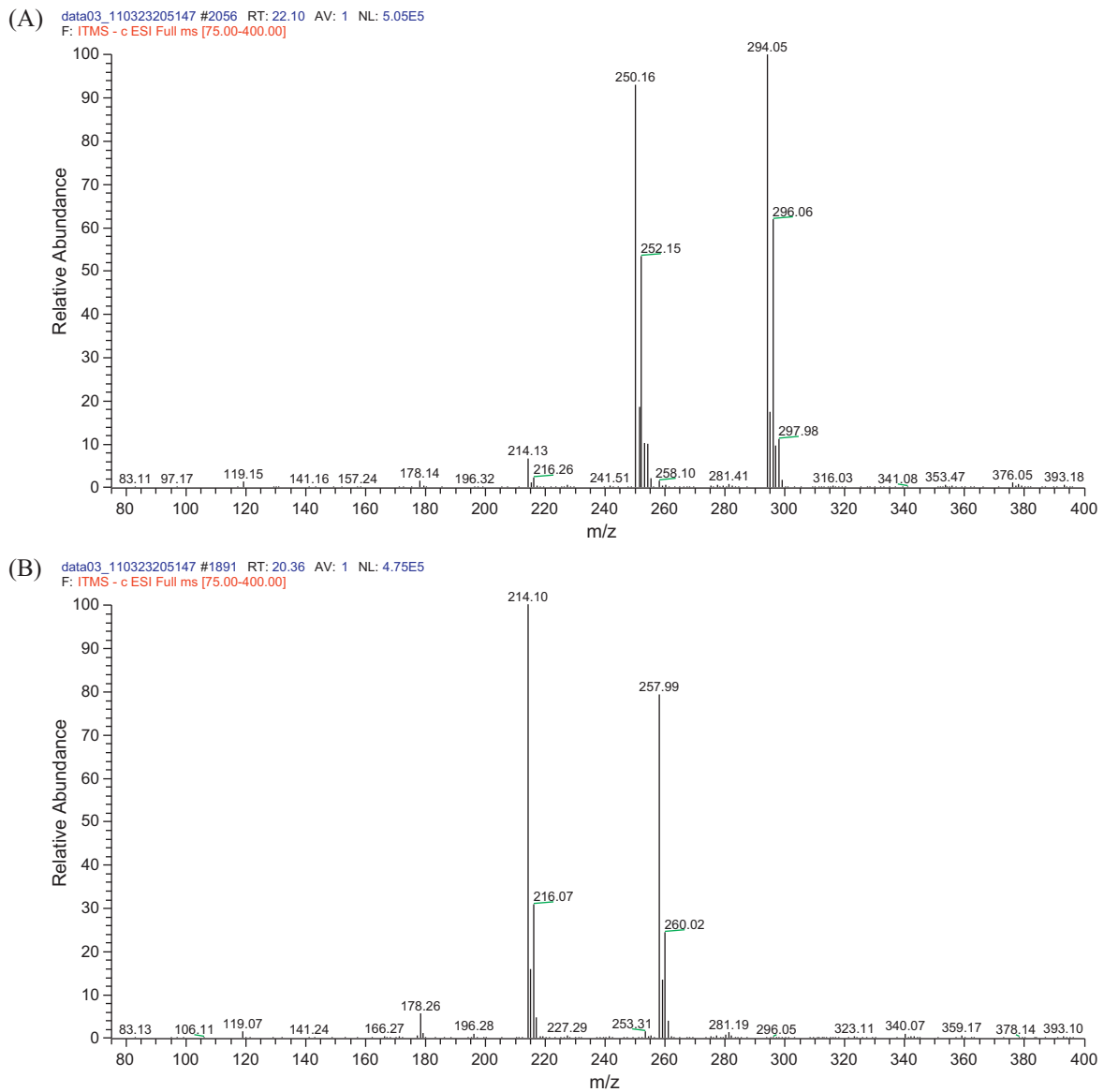


Fig. 6. LC-MS spectra of (A) diclofenac and (B) its PEC degradation intermediate.

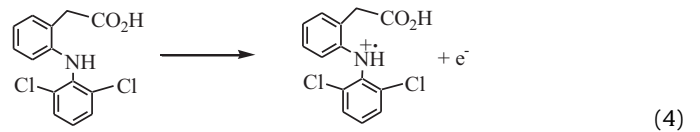
To understand the PEC degradation mechanism of diclofenac on this magnetic electrode, the main degradation intermediate after 60 min PEC treatment was separated by HPLC and identified with ESI-MS. Fig. 6 compares the LC/MS spectra of diclofenac and its PEC degradation intermediate. The mass spectrum of diclofenac produces a molecular ion at m/z 294 and a fragment ion at m/z 250 (Fig. 6A). While for the degradation intermediate of diclofenac, the spectrum shows a molecular ion at m/z 258 and a fragment ion at m/z 214 (Fig. 6B). The difference of 36 between the degradation intermediate and diclofenac is due to the loss of chlorine and hydrogen atoms, consistent with the proposal by Cavalheiro [44]. Based on this result, the mechanism of PEC oxidation of diclofenac by hydroxyl radical can be proposed. In the first step, photogenerated electrons and holes over TiO_2 are obtained when TSF is irradiated with UV light [45].



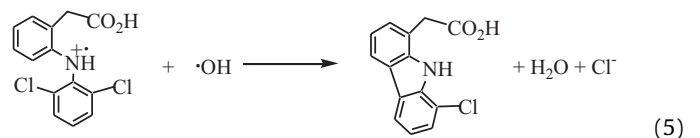
Then, holes react with H_2O or OH^- to form hydroxyl radicals.



While +0.8 V potential is applied, diclofenac is electro-oxidized on the TSF-loaded electrode to form a radical cation [46].



At the same time, the applied anodic bias potential drives photo-generated electrons to the counter electrode through the external electric circuit, which reduces the recombination of electrons and holes. Thus, more hydroxyl radicals according to reaction (2) or (3) are obtained to oxidize diclofenac radical cation.



Such an oxidation intermediate of diclofenac can undergo further reactions and ring cleavage to form small molecular derivatives under hydroxyl radical attack, which is eventually mineralized to CO_2 , Cl^- , H_2O and NH_3 .

4. Conclusions

Magnetic TSF core-shell nanoparticles were synthesized and loaded on the electrode surface with the aid of an external magnet. A series of experiments were carried out to study the PEC activity of magnetically attached TSF electrode. It was found that dispersant had a prominent effect on the performance of the prepared TSF electrode and the ethanol-dispersed TSF electrode showed high photoelectrochemical activity. For such a magnetic nanoparticles-loaded electrode, the external magnetic force kept TSF nanoparticles firmly adhered to the electrode and allowed efficient electron transfer between catalyst and electrode, leading to high PEC degradation efficiency and desirable stability during long-time degradation process. Based on this TSF-loaded electrode, effective PEC degradation of diclofenac was obtained. Our work demonstrates that magnetic loading of TSF nanoparticles on electrode surface provides a new strategy for preparing photoelectrochemical electrode with high stability, which could be applied to the PEC degradation of organic pollutants.

Acknowledgements

This work was supported by the National Natural Science Foundation of China (grant no. 20977037). The authors thank the Analytical and Testing Center of Huazhong University of Science and Technology for the help in surface analysis.

References

- [1] K. Pirkanneime, M. Sillanpaa, Heterogeneous water phase catalysis as an environmental application: a review, *Chemosphere* 48 (2002) 1047–1060.
- [2] A. Fujishima, T.N. Rao, D.S. Truk, Titanium dioxide photocatalysis, *J. Photochem. Photobiol. C* 1 (2000) 1–21.
- [3] D. Beydoun, R. Amal, G. Low, S. Mcevoy, Occurrence and prevention of photodissolution at the phase junction of magnetite and titanium dioxide, *J. Mol. Catal. A: Chem.* 180 (2002) 193–200.
- [4] T.A. Gad-Allah, K. Fujimura, S. Kato, S. Satokawa, T. Kojima, Preparation and characterization of magnetically separable photocatalyst ($\text{TiO}_2/\text{SiO}_2/\text{Fe}_3\text{O}_4$): effect of carbon coating and calcination temperature, *J. Hazard. Mater.* 154 (2008) 572–577.
- [5] S. Rana, R.S. Srivastava, M.M. Sorensson, R.D.K. Misra, Synthesis and characterization of nanoparticles with magnetic core and photocatalytic shell: anatase TiO_2 - NiFe_2O_4 system, *Mater. Sci. Eng. B* 119 (2005) 144–151.
- [6] F. Chen, Y. Xie, J. Zhao, G. Lu, Photocatalytic degradation of dyes on a magnetically separated photocatalyst under visible and UV irradiation, *Chemosphere* 44 (2001) 1159–1168.
- [7] Y. Gao, B. Chen, H. Li, Y. Ma, Preparation and characterization of a magnetically separated photocatalyst and its catalytic properties, *Mater. Chem. Phys.* 80 (2003) 348–355.
- [8] D.-K. Lee, I.-C. Cho, Characterization of TiO_2 thin film immobilized on glass tube and its application to PCE photocatalytic destruction, *Microchem. J.* 68 (2001) 215–223.
- [9] J.-M. Herrmann, H. Tahin, Y. Ait-Ichou, G. Lassalletta, A.R. González-Elipe, A. Fernández, Characterization and photocatalytic activity in aqueous medium of TiO_2 and Ag- TiO_2 coatings on quartz, *Appl. Catal. B: Environ.* 13 (1997) 219–228.
- [10] X. Cao, Y. Oda, F. Shiraishi, Photocatalytic and adsorptive treatment of 2,4-dinitrophenol using a TiO_2 film covering activated carbon surface, *Chem. Eng. J.* 156 (2010) 98–105.
- [11] M. Huang, C. Xu, Z. Wu, Y. Huang, J. Lin, J. Wu, Photocatalytic discolorization of methyl orange solution by Pt modified TiO_2 loaded on natural zeolite, *Dyes Pigm.* 77 (2008) 327–334.
- [12] N.J. Peill, M.R. Hoffmann, Mathematical model of a photocatalytic fiber-optic cable reactor for heterogeneous photocatalysis, *Environ. Sci. Technol.* 32 (1998) 398–404.
- [13] S. Horikoshi, N. Watanabe, H. Onishi, H. Hidaka, N. Serpone, Photodecomposition of a nonylphenol polyethoxylate surfactant in a cylindrical photoreactor with TiO_2 immobilized fiberglass cloth, *Appl. Catal. B: Environ.* 37 (2002) 117–129.
- [14] H. Liu, S. Cheng, M. Wu, H. Wu, J. Zhang, W. Li, C. Cao, Photoelectrocatalytic degradation of sulfosalicylic acid and its electrochemical impedance spectroscopy investigation, *J. Phys. Chem. A* 104 (2000) 7016–7020.
- [15] K. Vinodgopa1, V.S. Hotchandani, P.V. Kamat, Electrochemically assisted photocatalysis: titania particulate film electrodes for photocatalytic degradation of 4-chlorophenol, *J. Phys. Chem.* 97 (1993) 9040–9044.
- [16] J.M. Kesselman, N.S. Lewis, M.R. Hoffmann, Photoelectrochemical degradation of 4-chlorocatechol at TiO_2 electrodes: comparison between sorption and photoreactivity, *Environ. Sci. Technol.* 31 (1997) 2298–2302.
- [17] C. He, Y. Xiong, J. Chen, C. Zha, X. Zhu, Photoelectrochemical performance of Ag- TiO_2 /ITO film and photoelectrocatalytic activity towards the oxidation of organic pollutants, *J. Photochem. Photobiol. A* 157 (2003) 71–79.
- [18] C. Baumanis, D.W. Bahnemann, TiO_2 thin film electrodes: correlation between photocatalytic activity and electrochemical properties, *J. Phys. Chem. C* 112 (2008) 19097–19101.
- [19] E. Zacco, J. Adrian, R. Galve, M.-P. Marco, S. Alegret, M.I. Pividori, Electrochemical magnetosensing of antibiotic residues in milk, *Biosens. Bioelectron.* 22 (2007) 2184–2191.
- [20] Y.-Y. Lin, G. Liu, C.M. Wai, Y. Lin, Magnetic beads-based bioelectrochemical immunoassay of polycyclic aromatic hydrocarbons, *Electrochem. Commun.* 9 (2007) 1547–1552.
- [21] Y. Zhang, G. Zeng, L. Tang, D. Huang, X. Jiang, Y. Chen, A hydroquinone biosensor using modified core-shell magnetic nanoparticles supported on carbon paste electrode, *Biosens. Bioelectron.* 22 (2007) 2121–2126.
- [22] S. Qu, J. Wang, J. Kong, P. Yang, G. Chen, Magnetic loading of carbon nanotube/nano- Fe_3O_4 composite for electrochemical sensing, *Talanta* 71 (2007) 1096–1102.
- [23] C.G. Daughton, T.A. Ternes, Pharmaceuticals and personal care products in the environment: agents of subtle change? *Environ. Health Perspect.* 107 (1999) 907–938.
- [24] P. Calza, V.A. Sakkas, C. Medana, C. Baiocchi, A. Dimou, E. Pelizzetti, T. Albanis, Photocatalytic degradation study of diclofenac over aqueous TiO_2 suspensions, *Appl. Catal. B: Environ.* 67 (2006) 197–205.
- [25] I. Kim, H. Tanaka, Photodegradation characteristics of PPCPs in water with UV treatment, *Environ. Int.* 5 (2009) 793–802.
- [26] D. Vogna, R. Marotta, A. Napolitana, R. Andreozzi, M. d'Ischia, Advanced oxidation of the pharmaceutical drug of diclofenac with UV/ H_2O_2 and ozone, *Water Res.* 38 (2004) 414–422.
- [27] M. Ravina, L. Campanella, J. Kiwi, Accelerated mineralization of the drug diclofenac via Fenton reactions in a concentric photo-reactor, *Water Res.* 36 (2002) 3553–3560.
- [28] L.A. Pérez-Estrada, S. Malato, W. Gernjak, A. Agüera, E.M. Thurman, I. Ferrer, A.R. FernáNdez-Alba, Photo-Fenton degradation of diclofenac: identification of main intermediates and degradation pathway, *Environ. Sci. Technol.* 39 (2005) 8300–8306.
- [29] N.M. Vieno, H. Harkki, T. Tuhkanen, L. Kronberg, Occurrence of pharmaceuticals in river water and their elimination in a pilot-scale drinking water treatment plant, *Environ. Sci. Technol.* 41 (2007) 5077–5084.
- [30] M. Huber, S. Canonica, G.Y. Park, U. Von Gunten, Oxidation of pharmaceuticals during ozonation and advanced oxidation processes, *Environ. Sci. Technol.* 37 (2003) 1016–1024.
- [31] V. Naddeo, V. Belgiorno, D. Kassinos, D. Mantzavinos, S. Metric, Ultrasonic degradation, mineralization and detoxification of diclofenac in water: optimization of operating parameters, *Ultrason. Sonochem.* 17 (2010) 179–185.
- [32] J. Hartmann, P. Bartels, U. Mau, M. Witter, W.v. Tümpling, J. Hofmann, E. Nietzschmann, Degradation of the drug diclofenac in water by sonolysis in presence of catalysts, *Chemosphere* 70 (2008) 453–461.
- [33] X. Hu, J. Yang, C. Yang, J. Zhang, UV/ H_2O_2 degradation of 4-aminoantipyrine: a voltammetric study, *Chem. Eng. J.* 161 (2010) 68–72.
- [34] Z. Lei, X. Pang, N. Li, L. Lin, Y. Li, A novel two-step modifying process for preparation of chitosan-coated $\text{Fe}_3\text{O}_4/\text{SiO}_2$ microspheres, *J. Mater. Process. Technol.* 209 (2009) 3218–3225.
- [35] J. Wang, S. Zheng, Y. Shao, J. Liu, Z. Xu, D. Zhu, Amino-functionalized $\text{Fe}_3\text{O}_4/\text{SiO}_2$ core-shell magnetic nanomaterial as a novel adsorbent for aqueous heavy metals removal, *J. Colloid Interface Sci.* 349 (2010) 293–299.
- [36] J. Ji, P. Zeng, S. Ji, W. Yang, H. Liu, Y. Li, Catalytic activity of core-shell structured $\text{Cu}/\text{Fe}_3\text{O}_4/\text{SiO}_2$ microsphere catalysts, *Catal. Today* 158 (2010) 305.
- [37] Z. Lei, Y. Li, X. Wei, A facile two-step modifying process for preparation of poly(SStNa)-grafted $\text{Fe}_3\text{O}_4/\text{SiO}_2$ particles, *J. Solid State Chem.* 181 (2008) 480–486.
- [38] N. Mandzy, E. Grulke, T. Druffel, Breakage of TiO_2 agglomerates in electrostatically stabilized aqueous dispersions, *Powder Technol.* 160 (2005) 121–126.
- [39] I.G. Godinez, C.J.G. Darnault, Aggregation and transport of nano- TiO_2 in saturated porous media: effects of pH, surfactants and flow velocity, *Water Res.* 45 (2011) 839–851.
- [40] B.Y. Ahn, S.I. Seok, N.C. Pramanik, H. Kima, S.-I. Hong, Redispersible rutile TiO_2 nanocrystals in organic media by surface chemical modification with an inorganic barium hydroxide, *J. Colloid Interface Sci.* 297 (2006) 138–142.
- [41] A.L. Cui, T.J. Wang, H. He, Y. Jin, Dispersion behavior of ultrafine titanium dioxide particles in aqueous solution, *Chin. J. Proc. Eng.* 1 (2001) 99–101.
- [42] S. Lebrette, C. Pagnoux, P. Abéard, Stability of aqueous TiO_2 suspensions: influence of ethanol, *J. Colloid Interface Sci.* 280 (2004) 400–408.
- [43] J. Yang, X. Hu, J. Zhang, Voltammetric monitoring photodegradation of EDTA based on carbon nanotubes-modified electrode, *J. Hazard. Mater.* 181 (2010) 742–746.

- [44] A.A. Cavaleiro, J.C. Bruno, M.J. Saeki, J.P.S. Valente, A.O. Florentino, Photocatalytic decomposition of diclofenac potassium using silver-modified TiO₂ thin films, *Thin Solid Films* 516 (2008) 6240–6244.
- [45] T.A. Gad-Allah, S. Kato, S. Satokawa, T. Kojima, Treatment of synthetic dyes wastewater utilizing a magnetically separable photocatalyst (TiO₂/SiO₂/Fe₃O₄): parametric and kinetic studies, *Desalination* 244 (2009) 1–11.
- [46] R.N. Goyal, S. Chatterjee, B. Agrawal, Electrochemical investigations of diclofenac at edge plane pyrolytic graphite electrode and its determination in human urine, *Sens. Actuators B* 145 (2010) 743–748.